JOURNAL OF Applied Polymer SCIENCE

Conducting Polymer Coated Textile Based Multilayered Shields for Suppression of Microwave Radiations in 8.2–12.4 GHz Range

Parveen Saini,[1] Veena Choudhary[2]

[1]Polymeric and Soft Materials Section, CSIR-National Physical Laboratory, New Delhi-110 012, India

[2]Centre for Polymer Science and Engineering, Indian Institute of Technology, New Delhi-110 016, India

Correspondence to: P. Saini (E-mail: pksaini@nplindia.org)

ABSTRACT: Polypyrrole (PPY) based conducting textiles were prepared by *in situ* polymerization of pyrrole over cotton fabric. The SEM micrographs show smooth and uniform coating of PPY over fabric with only few loose dendrites. The elemental analysis and XRD patterns revealed the presence of iron whereas magnetization measurement shows ferromagnetic signature with well defined hysteresis loop and saturation magnetization (Ms) of 0.3 emu/g. The good antistatic property and rapid static charge dissipability was reflected by decay profile with decay time of only 0.16 sec. In addition, the microwave absorption studies of multilayered shields; made up of these conducting fabrics; show absorption dominated total shielding effectiveness (SE_T) value of −43.9 dB (i.e. >99.99% attenuation) which can be attributed to the better impedance matching, high microwave conductivity, shallow skin depth, and multiple scattering of incident electromagnetic radiation. © 2013 Wiley Periodicals, Inc. J. Appl. Polym. Sci. 000: 000–000, 2013

KEYWORDS: conducting polymers; thermogravimetric analysis (TGA); X-ray; textiles; magnetism and magnetic properties

Received 9 October 2012; accepted 6 January 2013; published online
DOI: 10.1002/app.38994

INTRODUCTION

The electromagnetic interference (EMI) which is an offshoot of rapidly growing field of electronics and instrumentation is becoming an alarming issue.[1] It is a novel kind of pollution which interferes with the normal functioning of electronic components and may lead to complete breakdown of appliance's performance. The consequences may be severe as loss of valuable money, energy, time, and even precious human life. Therefore, some blocking mechanism must be provided to protect the concerned article from these spurious electromagnetic (EM) noises. The EM radiation checking regulations become even sterner when sensitive areas like defense, space and medicine are concerned.[2,3] In this regard, conducting polymers with finite conductivity and non-transparency to microwaves can extend an attractive solution for effective handling of EM pollution.[4–8] Particularly, the synthetic metals like polyaniline (PANI) and polypyrrole (PPY) based compositions have received world wide attention due to their promising applications in wide spread areas like organic light emitting diodes, solar cells, electro chromic devices, sensors, battery electrodes, EMI shielding and microwave absorption.[9–15] Recently, several attempts have been made to design the conducting polymer coated fabrics as flexible and large area EM shield.[16–18] These fabrics combine the mechanical properties, stitch-ability and flexibility of fabrics with conductivity of doped π-conjugated polymers.[19,20] Interestingly, the direct coating of conducting polymers on the surface of textiles via *in-situ* polymerization route even eliminates the need of thermal or solution processability. These fabrics also provide good electrostatic charge dissipation (ESD) in addition to EM radiation blocking response. In this regard, several attempts have been made in the past to produce coatings of conducting polymers over fabrics but the achieved shielding efficiencies were remained rather low due to low conductivity, leakage of radiation from the microwave transparent empty spaces (voids) between fabric weaves and absence of any secondary shielding mechanism. The present work explores the microwave absorption property of the multilayered shield made by stacking different layers of PPY coated fabrics, and discusses the effect of stacking on the shielding effectiveness. Since both conducting as well as magnetic properties are important;[3,21] therefore, we selected $FeCl_3$ doped PPY as a conducting polymer with inherent ferromagnetic behavior. Further, the above fabrics were deliberately assembled in the form of layered structures in order to induce multiple scattering (and associated multiple absorptions) as well as to reduce the radiation transparent empty spaces between the weaves of woven fabrics. The EM attributes of the shield i.e. complex permittivity and permeability have also been measured alongwith skin depth and microwave conductivity. The synthesized materials were also characterized by specific probes like Fourier transform-infrared (FT-

IR) spectroscopy, X-ray diffraction (XRD), scanning electron microscopy (SEM) and thermogravimetric analysis (TGA), two-probe conductivity setup, and JCI static charge decay test (CDT) unit so as to complement and explain the observed results.

EXPERIMENTAL

Materials Used

Pyrrole (Fluka Chemika, India) was freshly double distilled before use. Anhydrous ferric chloride ($FeCl_3$ Qualigens, India) was used without further purification. Aqueous solutions were prepared from the double distilled water having specific resistivity of 10^6 Ohm-cm.

Preparation of Polypyrrole-Coated Fabrics

Polypyrrole (PPY)-coated fabrics were prepared by *in situ* chemical oxidative polymerization[18] using $FeCl_3$ as oxidant. The cotton fabric (15 cm × 15 cm) was placed in a glass trough containing 200 mL aqueous solution of 0.1*M* pyrrole. The polymerization was initiated by the drop wise addition of 0.2*M* aqueous solution of $FeCl_3$ added over a period of 2 h. The temperature of the reaction mixture was maintained at 23°C with uninterrupted agitation throughout the course of reaction (2 h). After, completion of polymerization, the polypyrrole grafted fabric (Cotton-PPY) was removed from the trough, thoroughly rinsed with distilled water & chloroform and dried at 60°C under vacuum.

Structural Characterization

The room temperature conductivity of coated fabric was measured by two-probe technique using programmable current source (Keithley-220) and a nanovoltmeter (Keithley-181). The identification of cellulosic and PPY phases in the composite was done by taking infrared spectra of the samples at resolution of 4.0 cm^{-1} in 4000 to 500 cm^{-1} range using FT-IR spectrophotometer (NICOLET 5700) and diamond ATR accessory. The phase identification was performed using X-ray diffractometer (XRD, Brooker Advanced D8 system) in the diffraction (2θ) range of 20 to 80°. The measurements were taken at scan rate of 0.02°/sec, slit width of 0.1 mm and using Cu-Kα (λ = 1.540598Å) radiation source. The thermal stability was measured under inert atmosphere of nitrogen using TGA (Mettler Toledo TGA/SDTA 851^e) and heating the materials from 298 to 973°K at thermal ramp of 10°C/min. The weight loss was continuously monitored as a function of temperature. The measurement of static decay time of the conducting fabric was done using charge decay test unit (John Chubb Instrument, UK, Model-JCI-155v5). Both shielding effectiveness (SE) as well as electromagnetic attributes (complex permittivity and permeability) were measured using a vector network analyzer (VNA E8263BAgilent Technologies) by keeping the samples in a sample holder placed between flanges of X-band (8.2–12.4 GHz) waveguidesand and keeping the input power level at -5dBm. The magnetic measurements were performed using vibrating sample magnetometer (VSM), Model 7304, Lakeshore Cryotronics Inc.

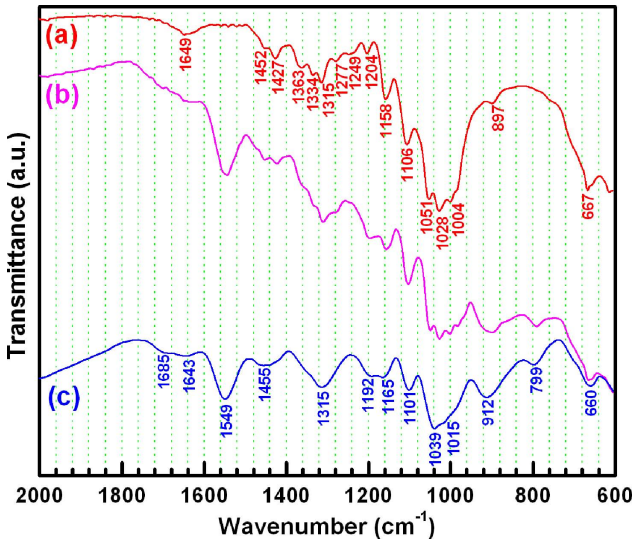

Figure 1. FT-IR spectra of (a) pure (uncoated) cotton fabric, (b) cotton fabric coated with polypyrrole, and (c) pure polypyrrole powder. [Color figure can be viewed in the online issue, which is available at wileyonlinelibrary.com.]

RESULTS AND DISCUSSION

FT-IR Measurements

Figure 1 shows the FTIR spectra of PPY powder as well as uncoated (blank) and PPY coated cotton fabrics. The pure cotton fabric [Figure 1(a)] shows the characteristic bands of cellulose[22] located at 1649, 1452, 1427, 1363, 1334, 1315, 1277, 1249, 1204, 1158 ,1106, 1051, 1028, 1004, 897, 667 cm^{-1}. In contrast, the main FTIR vibrations of PPY [Figure 1(c)] are located at 1685, 1643, 1549, 1455, 1315, 1192, 1165, 1101, 1039, 1015, 912, 799, and 660 cm^{-1}. On coating with conducting polymer, the superimposed bands of PPY and cotton [Figure 1(b)] were observed. In particular, the appearance of characteristic bands at 1548 (C=C stretching), 1456 (C-C stretching), 1314 (C-N stretching), 1191 (C=N stretching), 1102 cm^{-1} (N-H in plane bending), 1040 (N-H wagging), and 798 cm^{-1} (C-H out-of-plane bending) confirm the formation of conducting PPY coating over cotton fabric.

XRD Studies

Figure 2(a,b) shows the X-ray diffraction patterns of uncoated and PPY coated cotton fabrics respectively. The pure cotton gives a sharp peak at 2θ values of 22.8° (d = 3.90 Å) and a broad hump (weak) at 2θ = 34.2° (d = 2.62 Å), which represents the characteristic signature of cellulosic structure[23] and match with its standard XRD pattern (JCPDS No. 50-2241). On the other hand, the PPY coated fabric shows distinct peaks at 2θ values of 26.9° and 49.2° in addition to the characteristic peaks of cellulose. The diffraction signal at 26.9° originated from the inter-planar scattering by PPY chains whereas the 49.2° peak was contributed by the iron present in $FeCl_4^-$ counter-ion.[24] The above results confirm the formation of doped PPY chains over cotton fibers.

Morphological and Magnetization Investigations

Figure 3(a,b) shows SEM images of the pure cotton and PPY grafted cotton, respectively. Pure cotton (uncoated) has a

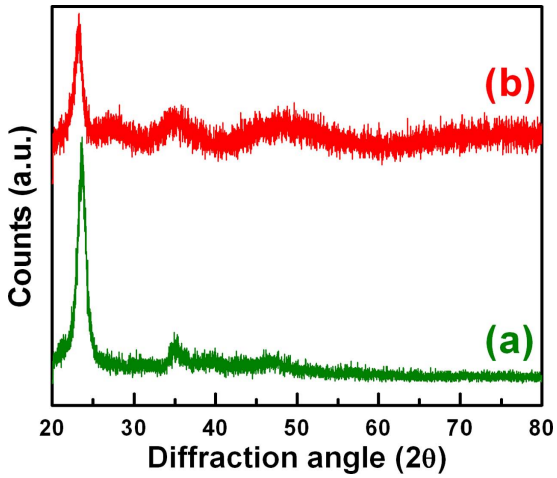

Figure 2. XRD of (a) pure cotton fabric and (b) cotton fabric coated with polypyrrole showing the formation of PPY. [Color figure can be viewed in the online issue, which is available at wileyonlinelibrary.com.]

collapsed tubular morphology with smooth surface, whereas PPY coated cotton clearly shows the presence of thin (and smooth) electrically conducting (brighter) layer of PPY over the surface individual fibers. The image also revealed that nodular growth due to the uncontrolled bulk polymerization was suppressed and only few non-adherent nodules were formed. Figure 3(c) shows the energy dispersive X-ray spectroscopy analysis (EDS) of coated fabric which clearly shows peaks corresponding to the elemental presence of C, O (from Cotton and PPY), N (from PPY), and Fe, Cl (from ferric dopant). The presence of iron imparts ferromagnetic characteristic to the doped PPY which can be clearly seen as hysteresis loop in VSM plot [Figure 3(d)]. The saturation magnetization (Ms), remnant magnetization (Mr) and coercivity (Hc) of the polypyrrole particles were found to be 0.3 emu/g, 0.04 emu/g, and 85.0 G respectively. The presence of hysteresis loop indicates the electromagnetic energy absorption and dissipation capability of these materials. In fact, good magnetic properties are expected to improve the microwave attenuation efficiency[21] due to better impedance matching, suppression of reflection loss and reduction of skin depth leading to enhancement of absorption phenomenon.

Thermogravimetric Analysis (TGA)

The thermogravimetric (TG) trace of PPY-$FeCl_3$ powder [Figure 4(a)] displays a continuous mass loss in the entire temperature range with ~40% weight loss. In contrast, the TG traces [Figure 4(b)] of uncoated cotton fabric (CF) and PPY coated cotton fabric (CFPY) show a systematic and stepwise weight loss in the concerned temperature range. The first small weight step around 393 K (120°C) is due to the superficially adsorbed water molecules or any other volatile moieties. Afterward, CF exhibit good thermal stability upto 573 K (300°C). Thereafter, the observed degradation of cotton was marked by abrupt weight loss of ~80%. On the other hand, CFPY shows an additional (apart from the loss step of CF) weight loss at 473 K (200°C) due to loss of dopant moiety ($FeCl_4^-$) as well as

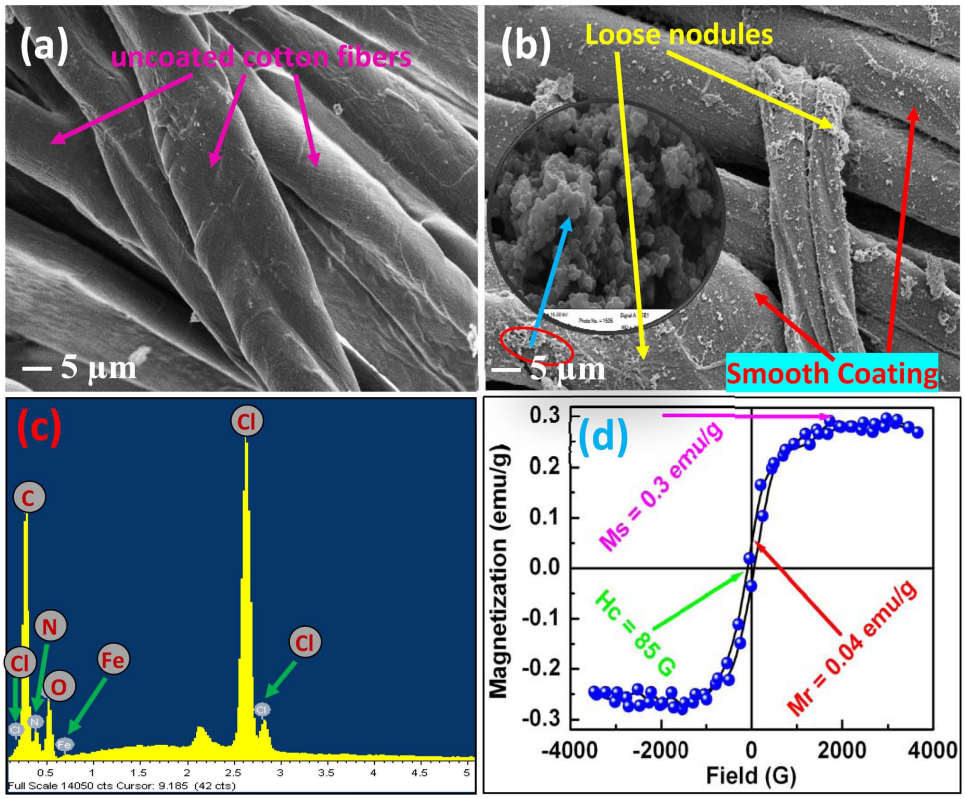

Figure 3. SEM pictures of (a) pure cotton fabric (CF), (b) polypyrrole coated fabric (CFPY), (c) elemental analysis of CFPY, and (d) magnetic parameters of coated polypyrrole particles. [Color figure can be viewed in the online issue, which is available at wileyonlinelibrary.com.]

Applied Polymer SCIENCE

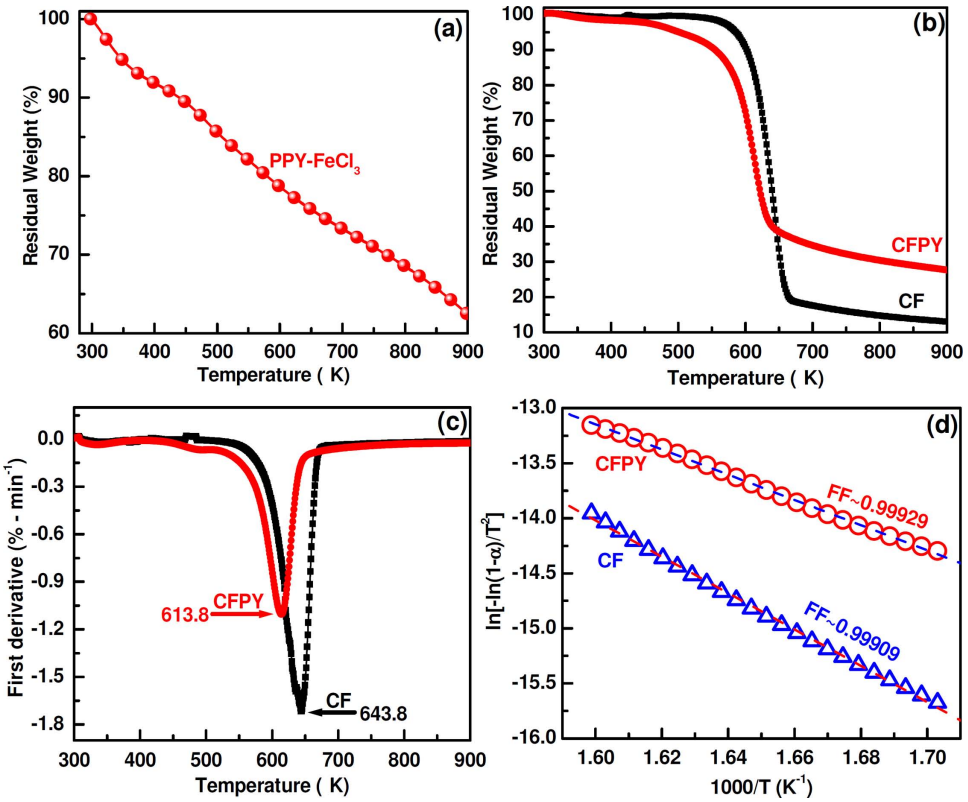

Figure 4. TG traces of (a) pure PPY and (b) CF and CFPY, (c) DTG traces of CF and CFPY, (d) Redfern-Coats kinetic plots of CF and CFPY. [Color figure can be viewed in the online issue, which is available at wileyonlinelibrary.com.]

onset of degradation of coated PPY phase. However, like pure cotton, major weight loss occurs only after 300°C, that can aptly be associated with the degradation of cotton backbone. The first derivative or DTG (differential thermogravimetric) trace of samples [Figure 4(c)] show that CF gives a maximum loss rate peak at 643.8 K whereas CFPY gives peak at 30 K less temperature (i.e. at 613.8 K). Further, the preliminary information about extent of coating can be estimated by observing the amounts of residual char. The char residue difference between cotton (CF) and cotton-ppy (CFPY) was found to be 9.9 wt % which is quite close to the weight gain (9.5 wt %) during coating of PPY by *in situ* polymerization. The degradation kinetic studies were also performed to get the estimation of associated kinetic parameters. The activation energy can be computed from the knowledge of initial decomposition temperature (IDT) for a given heating rate and temperature range. The kinetic analysis of polymer degradation begins with the following fundamental differential rate equation:

$$\frac{d\alpha}{dt} = k(1-\alpha)^n \tag{1}$$

where α is the fraction of material decomposed at any time t and n is the order of reaction. The proportionality or rate constant k for an non-isothermal system can be further expressed as:

$$k = k_o \exp\left(-\frac{E_a}{RT}\right) \tag{2}$$

where k_o is pre-exponential factor, E_a is activation energy, R is universal gas constant (8.314 J/K) and T is absolute temperature in Kelvin. Therefore, under non-isothermal conditions, the kinetics of heterogeneous condensed phase reactions as obtained by combining eqs. (1) and (2) and introducing heating rate ($\beta = dT/dt$) , can be expressed as:

$$\frac{d\alpha}{dT} = \frac{k_o}{\beta}\exp\left(-\frac{E_a}{RT}\right)(1-\alpha)^n \tag{3}$$

Based on above expression i.e. [eq. (3)], numerous methods (and related equations) have been developed under suitable assumptions, in order to retrieve the kinetic triplets i.e. E_a, n, and k_o from given thermogravimetric plot. The values of above triplets depends upon several factors like environment (i.e. inert or reactive), sample shape and weight, gas flow rate, heating rate, and the kind of mathematical approach used to process the TGA data. In the present study we used the integral method i.e. analysis of Coats and Redfern[25] that give the solutions of eq. (3) as:

$$\ln\left[\frac{1-(1-\alpha)^{(1-n)}}{T^2(1-\alpha)}\right] = \ln\frac{k_0 R}{\beta E_a}\left[1-\frac{2RT}{E_a}\right] - \frac{E_a}{RT} \quad for \quad n \neq 1 \tag{4}$$

$$\ln\left[\frac{-\ln(1-\alpha)}{T^2}\right] = \ln\frac{k_0 R}{\beta E_a}\left[1-\frac{2RT}{E_a}\right] - \frac{E_a}{RT} \quad for \quad n = 1 \tag{5}$$

Therefore, from the knowledge that degradation of cotton is a unimolecular reaction with order equals to unity (i.e. $n = 1$), we used eq. (5) for fitting TGA data. Figure 4(d) shows the Redfern-Colt plots of left hand side of eq. (5) against $1000/T$ for pure cotton and cotton-ppy fabrics, respectively. The plots were found to be linear and the slope of their straight line fits give value of term $E_a/1000R$. Therefore, E_a value was found to be 137.2 kJ/mol K and 95.2 kJ/mol K for CF and CFPY fabrics respectively.

Electrical Conductivity and Antistatic Studies

The room temperature electrical conductivity of polypyrrole coated fabric has been found to be 4.3×10^{-3} S/cm, which conforms to the conductivity range (10^{-9}–10^{-5} S/cm) specified in the Electronics Industries Association (EIA) standard for ensuring efficient dissipation of electrostatic charges.[26] The static charge decay profiles (Figure 5) of the above fabrics were recorded using JCI static charge decay unit for corona charging voltages of ±5.0 kV. The results show that accepted charge decays in an exponential manner marked by a sharp initial decay followed by a plateau region. The results show that blank cotton gives a peak at 150.09 V which indicates that cotton accepted only ~3.0% of the applied voltage (5.0 kV). Further, the accepted surface voltage decays to 10% cur-off limit in 3.54 sec. that was higher than limiting time of 2.0 sec. Such a low dissipation rate can be ascribed to the inherent insulating nature of the cotton. However, on coating cotton with conducting PPY, charge acceptability and retention capability drastically decreases, due to rapid charge dissipation. Therefore, PPY coated fabric accepted only 43.4 V of applied corona voltage (5.0 kV), which rapidly decays and reaches 10% cut-off limit within 0.16 sec. The above decay time value is much less than the antistatic criteria of 2.0 sec and ensures efficient ESD performance of fabric under service conditions. The good antistatic response of these textiles arises due to coated fiber that forms conducting domains having high aspect ratio accruing from the long lengths of individual fibers. The weaved fabric further

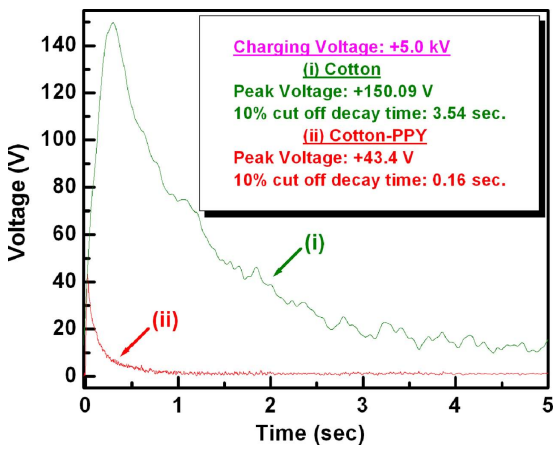

Figure 5. Static decay profiles of (a) pure cotton and (b) PPY coated conducting fabric, showing the exponential charge decay, accepted voltage/charge and decay time. [Color figure can be viewed in the online issue, which is available at wileyonlinelibrary.com.]

enhances the charge transport due to formation of continuous network of interconnected conducting fibers over whole surface of fabric. The aforementioned acceptable conductivity as well as inherent magnetic properties suggests that these coated fabrics are also expected to exhibit good microwave attenuation efficiency for which recommended conductivity range is 10^{-3} to 0.1 S/cm.[27]

The shielding efficiency is conveniently measured in terms of quantity called shielding effectiveness which is defined as the attenuation of the propagating electromagnetic (EM) waves produced by the shielding material. The EMI shielding is a direct consequence of reflection, absorption, and multiple internal reflection losses at the existing interfaces, suffered by incident electromagnetic (EM) waves. The total shielding effectiveness (SE_T) that includes contributions due to reflection and absorption can be expressed as:[28,29]

$$\begin{aligned} SE_T(dB) &= 10\log_{10}(P_T/P_I) = 20\log_{10}(E_T/E_I) \\ &= 20\log_{10}(H_T/H_I) \end{aligned} \quad (6)$$

where P_I (E_I or H_I) and P_T (E_T or H_T) are the power (electric or magnetic field intensity) of incident and transmitted EM waves, respectively. The Scattering parameters S_{11} (S_{22}) and S_{12} (S_{21}) of VNA are related to reflectance (R) and transmittance (T) respectively i.e. $T = |E_T/E_I|^2 = |S_{12}|^2$ ($=|S_{12}|^2$), $R = |E_R/E_I|^2 = |S_{11}|^2$ ($=|S_{22}|^2$). Once, the values of "R" and "T" are known, absorbance (A) can be calculated as: $A = (1 - R - T)$. Further, the relative intensity of the EM wave inside the shield (after primary reflection from the face of incidence) is based on the quantity $(1 - R)$ and effective absorbance (A_{eff}) can be described as $A_{eff} = (1 - R - T)/(1 - R)$. Therefore, attenuations due to reflection (SE_R) and absorption (SE_A) can be conveniently expressed as:

$$SE_R = 10\log_{10}(1 - R) \quad (7)$$

$$SE_A = 10\log(1 - A_{eff}) = 10\log_{10}[T/(1 - R)] \quad (8)$$

According to classical EM wave theory, far field ($kr >> 1$) losses for good conductor[30] ($\sigma_T/\omega\varepsilon_o > 0$) and electrically thick samples ($t > \delta$), angular frequency (ω) dependence of reflection and absorption losses can be expressed in the terms of total conductivity (σ_T), real permeability (μ'), skin depth (δ), and thickness (t) of the shield material as:[8,30]

$$SE_R(dB) = -10\ \log_{10}\left(\frac{\sigma_T}{16\omega\varepsilon_o\mu'}\right) \quad (9)$$

$$SE_A(dB) = -20\frac{t}{\delta}\log_{10}\ e = -8.68\left(\frac{t}{\delta}\right) \quad (10)$$

$$\sigma_T = (\sigma_{ac} + \sigma_{dc}) = \omega\varepsilon_0\varepsilon'' \quad (11)$$

where σ_{ac} and σ_{dc} are frequency dependent (ac) and independent (dc) components of σ_T whereas ε is imaginary permittivity "k" is wave number and "r" is distance between radiation source and detector. The skin depth (δ) is defined as the depth of penetration at which the incident EM radiation is reduced to 33% of its original strength and can be expressed in terms of real

permeability (μ'), σ_T and ω as $\delta = \left\{\frac{2}{\sigma_T \omega \mu'}\right\}^{\frac{1}{2}}$ which gives absorption loss as:

$$SE_A(dB) = -8.68t\left(\frac{\sigma_T \omega \mu'}{2}\right)^{\frac{1}{2}} \quad (12)$$

The above equations revealed that both conductivity as well as magnetic properties are important, therefore, we used $FeCl_3$ doped PPY as a conducting polymer with inherent magnetic behavior. Figure 6(a) shows that total shielding effectiveness (SE_T) for a single layer (layer 1) of fabric was around −10.6 dB which corresponds to ~93% attenuation. However, on increasing the thickness by adding successive layers of coated fabrics, the total shielding reaches upto −45.7 dB, for a shield containing five layers (layer 5). To probe further, the SE_T was separated into two components i.e. losses due to absorption and reflection. Figure 6(b) shows that for a given sample, reflection loss (SE_R) has decreasing trend with increase in frequency. On the other hand, absorption loss (SE_A) shows [Figure 6(c)] monotonous increase with increase in frequency. This can be attributed to the dispersion phenomenon [i.e. variation of complex permittivity and permeability with frequency, Figure 6(d)] and increase in microwave conductivity [σ_T, Figure 6(e)], leading to decrease in skin depth [Figure 6(f)]. The EM attributes i.e. complex permittivity ($\varepsilon' - j\varepsilon''$) and permeability ($\mu' - j\mu''$) were also obtained from experimental S parameters (S_{11} or S_{22} and S_{12} or S_{21}) using standard Nicolson-Ross-Weir (NRW) technique.[31,32] The real permittivity (ε') or dielectric constant represents the charge storing capacity whereas the imaginary permeability (ε'') is a measure of dielectric losses. Similarly magnetic storage and losses were represented by the magnetic

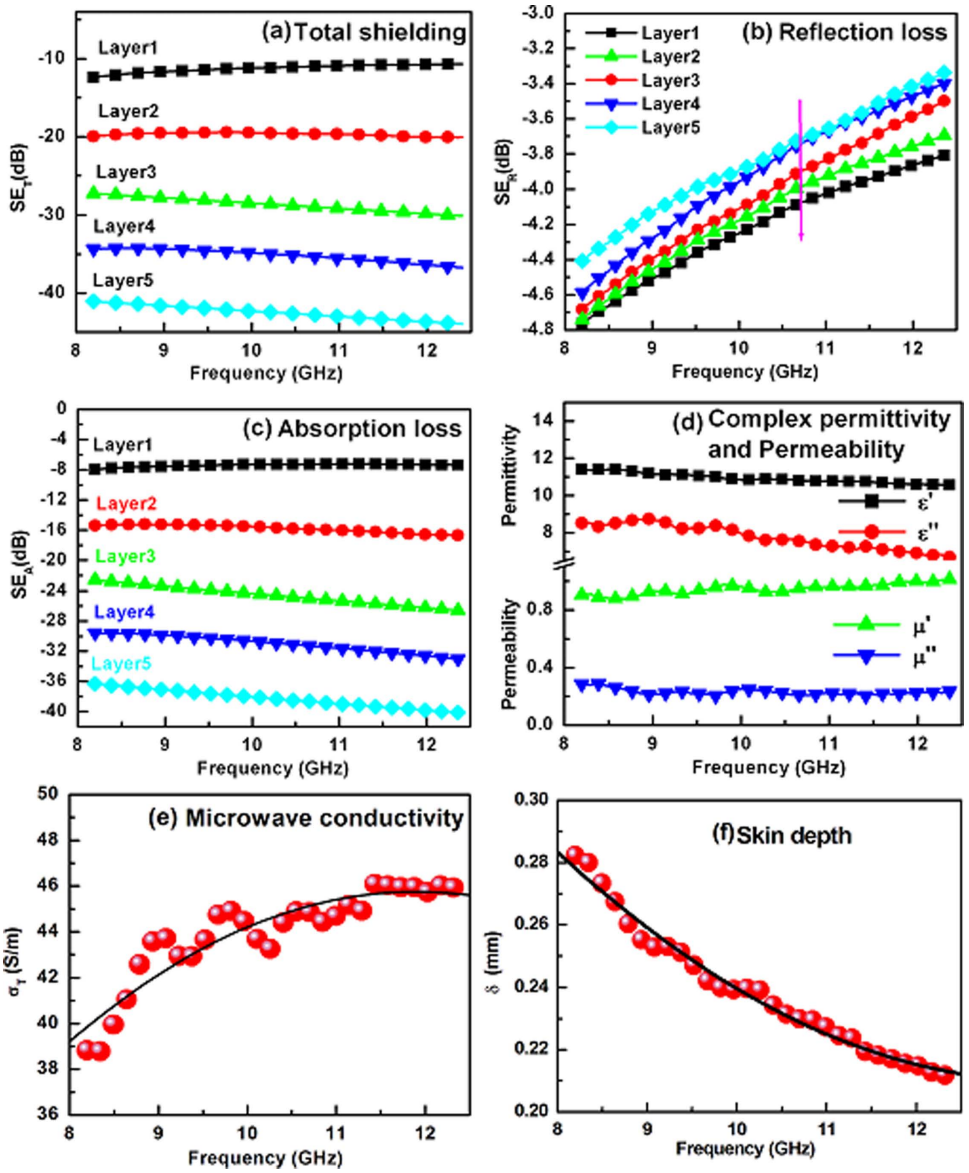

Figure 6. Frequency dependence of (a) total shielding (SE_T), (b) reflection loss (SE_R), (c) absorption loss (SE_A), (d) complex permittivity (ε^*)/permeability (μ^*), (e) microwave conductivity (σ_T) and (f) skin depth (δ) of polypyrrole coated fabrics. [Color figure can be viewed in the online issue, which is available at wileyonlinelibrary.com.]

permeability's real (μ') and imaginary (μ'') parts. The formation of localized polarons and bipolarons on PPY chains leads to pronounced polarization effects. The space charge formation due to conductivity difference between PPY and cotton also contributes towards interfacial polarization. These effects and associated losses are responsible for high values of ε' and ε''. Figure 6(d) shows that with the increase in frequency, dielectric constant (ε') decreases from 11.4 to 10.6 whereas the loss factor (ε'') decreases from 8.5 to 6.7. In contrast, real permeability (μ') increases slightly [Figure 6(d)] from 0.9 to 1.02 and the magnetic losses (μ'') varies from 0.28 to 0.24. Both eddy currents (due to conducting nature of PPY) as well as ferromagnetism (from $FeCl_4^{-1}$ counter ion of dopant) were responsible for observed magnetic losses. Therefore, the good electromagnetic response of these coated fabrics can be ascribed to the combination of good dielectric and magnetic properties.

Further, as the shield thickness was increased by successive stacking of fabric layers, the multiple reflection phenomena (shown schematically in Figure 7) sets in due to poor impedance matching at interface of each layer. The consequent re-reflections result in multiple passes of radiation between two opposing faces of the stacked shield. Each of these passes results in associated absorptions step contributing toward total absorption. Therefore, total absorbance (A) can be visualized as a combined effect of above multiple absorption sub-steps, resulting in higher attenuation due to absorption. Further, due to the porous nature of the fabrics, the multiple scattering also takes place between conducting microdomains. As the shield thickness increases by successive stacking of the fabric layers, amount of conducting polymer present within the bulk of shield (i.e. on the surface and pores of fabric) increases. Therefore, the total number of conducting and reflecting planes that are present between two extreme faces of the shield also increases. The phenomena of partial absorption, transmission, and multiple reflections are repeated in each subsequent layer resulting in more effective interception of radiation by the shield and corresponding enhancement of absorption within the bulk of the sample. The free spaces between the fibers in weaved fabrics do not contributes towards attenuation and allow the incident electromagnetic radiation to pass through shield unperturbed. This reduces the overall attenuation level due to reduction of reflection and absorption loss (SE_A) losses. The layered structures reduce these microwave transparent empty spaces as the conducting fibers of one layer covers the voids of other layer. Further, though the total shielding effectiveness increases with number of layers, the underlying reflection loss is expected to remain constant, as it is directly related to conductivity [eq. (9)] which is same for all the layers. However, the experimental reflection loss did not remain constant and a small but noticeable rise in it could be registered. This can be attributed to the contributions from multiple reflections to the total reflectance (R) that has been registered at the EM wave incident face of the first layer. However, due to the associated multiple absorption loss steps, the EM wave power decreases in magnitude each time the radiation passes through the thickness of the shield. Therefore, these multiply reflected components of radiation already decreased in intensity (reduced in magnitude) before reaching the left face of the first layer. Consequently, the contribution towards (R) comes chiefly from primary reflection and secondary reflections (Figure 7) give only nominal contribution. In addition, absorption loss is a bulk related phenomenon whereas the reflection is a surface effect and occurs due to interaction of incident waves with free electrons of the shield. As the stacking of layers leads to rapid fall of surface (i.e. area of radiation incident face) to bulk (i.e. volume of layered stack) ratio, therefore, on stacking the attenuation due absorption increases by much larger magnitude than the reflection loss. Similarly, although the multiple reflections also contribute toward enhancement of SE_R but its effect is more prominent on SE_A.

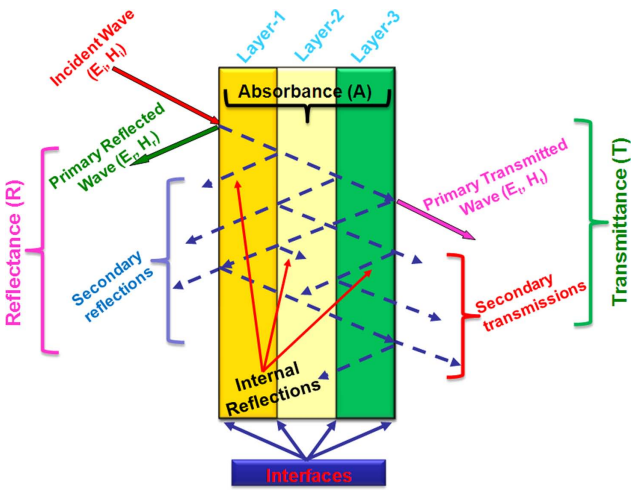

Figure 7. Schematic of the multilayered shield showing reflection, absorption, re-reflection inside individual layer, and its cumulative effect across shield. [Color figure can be viewed in the online issue, which is available at wileyonlinelibrary.com.]

CONCLUSIONS

Polypyrrole (PPY) based conducting textiles were prepared to extend microwave shielding capability alongwith antistatic action. The SEM images show smooth uniform coating of PPY over fabric with only few loose dendrites whereas FT-IR confirms the formation of PPY coating. TGA shows slight deterioration of thermal stability of cotton after coating with PPY whereas Redfern-Colts kinetic analysis gives the values of E_a as 137.2 kJ/mol K and 95.2 kJ/mol K for CF and CFPY, respectively. These fabrics show enough conductivity to immediately dissipate any static charge with decay time much less (~0.16 sec) than antistatic criteria of 2.0 sec. The elemental analysis and XRD patterns revealed the presence of iron within polymer matrix which is responsible for inherent magnetic properties. The VSM measurement of coated polymer shows the presence of ferromagnetic signature with well defined hysteresis loop and saturation magnetization (Ms) value of 0.3 emu/g, accounting for good absorption response. The X-band (8.2–12.4 GHz) microwave absorption studies of multilayered shields made up of these conducting fabrics show absorption dominated total shielding effectiveness value of −43.9 dB (i.e. >99.99% attenuation) for a five-layered structure. The enhanced absorption arises due to better impedance matching, high

microwave conductivity, low skin depth, good magnetic properties and multiple scattering of incident electromagnetic radiation. The observed high value of attenuation supports its candidature as a promising microwave absorbing material.

ACKNOWLEDGMENTS

The authors thank Director CSIR-NPL for his keen interest in the work. The authors are also thankful to Dr. R.K. Kotnala for VSM study, Mr. K.N Sood for recording the SEM micrographs and Dr. N. Vijayan for XRD patterns. Technical suggestions by Dr. S. K. Dhawan are gratefully acknowledged.

REFERENCES

1. Saini, P.; Choudhary, V. *J. Mater. Sci.* **2013**, *48*, 797.
2. John, D.; Washington, M. *Aviat Week Space Technol.* **1998**, *129*, 28.
3. Saini, P.; Arora, M. New Polymers for Special Applications; Intech: Croatia, **2012**. doi:10.5772/48779; Available at: http://www.intechopen.com/download/pdf/38964
4. Kulkarni, V. G.; Mathew, W. R.; Campbell, J. C.; Dinkins, C. J.; Durbin, P. J. *ANTEC Conf. Proc.* **1991**, *37*, 663.
5. MacDiarmid, A. G.; Epstein, A. J. *MRS Symp. Proc.* **1994**, *328*, 133.
6. Chandrasekhar, P.; Naishadham, K. *Synth. Met.* **1999**, *105*, 115.
7. Cao, Y.; Smith, P.; Heeger, A. J. *Synth. Met.* **1992**, *48*, 91.
8. Saini, P.; Choudhary, V.; Singh, B. P.; Mathur, R. B.; Dhawan, S. K. *Synth. Met.* **2011**, *161*, 1522.
9. Gustafsson, G.; Cao, Y.; Treacy, G. M.; Colaneri, N. F.; Heeger, A. J. *Nature* **1992**, *357*, 477.
10. Tan, S.; Zhai, J.; Xue, B.; Wan, M.; Meng, Q.; Li, Y.; Jiang, L.; Zhu, D. *Langmuir* **2004**, *20*, 2934.
11. Sonavane, A. C.; Inamdar, A. I.; Deshmukh, H. P.; Patil, P. S. *J. Phys. D: Appl. Phys.* **2010**, *43*, 315102.
12. Gong, J.; Li, Y.; Hu. Z.; Zhou, Z.; Deng, Y. J. *Phys. Chem. C* **2010**, *114*, 9970.
13. Zhang, H.; Cao, G.; Wang, Z.; Yang, Y.; Shi, Z.; Gu, Z. *Electrochem. Sol. Stat. Lett.* **2008**, *11*, A223.
14. Saini, P.; Choudhary V.; Dhawan S. K. *Polym. Adv. Technol.* **2009**, *20*, 355.
15. Makeiff, D. A.; Huber, T. *Synth. Met.* **2007**, *156*, 917.
16. Abbas, S. M.; Dixit, A. K.; Chatterjee, R.; Goel, T. C. *J. Nanosci. Nanotechnol.* **2007**, *7*, 2129.
17. Hakansson, E.; Amiet, A.; Kaynak, A. *Synth. Met.* **2006**, *156*, 497.
18. Saini, P.; Choudhary, V.; Dhawan, S. K. *J. Appl. Polym. Sci.* **2012**, *23*, 343.
19. Seshadri, D. T.; Bhat, N. V. *Sen'i Gakkaishi* **2005**, *61*, 103.
20. dall'Acqua, L.; Tonin, C.; Peila, R.; Ferrero F.; Catellani, M. *Synth. Met.* **2004**, *146*, 213.
21. Saini, P.; Choudhary, V.; Vijayan, N.; Kotnala, R. K. *J. Phys. Chem. C* **2012**, *116*, 13403.
22. Konyushenko, E. N.; Stejskal, J.; Trchova, M.; Hradil, J.; Kovarova, J.; Prokes, J.; Cieslar, M.; Hwang, J. -Y.; Chen K. -H.; Sapurina, I. *Polymer* **2006**, *47*, 5715.
23. Zhao, H.; Kwak, J. H.; Zhang, Z. C.; Brown, H. M.; Arey, B. W.; Holladay, J. E. *Carbohydr. Polym.* **2007**, *68*, 235.
24. Selvaraj, M.; Palraj, S.; Maruthan, K.; Rajagopal, G.; Venkatachari, G. *Synth. Met.* **2008**, *158*, 888.
25. Coats, A. W.; Redfren, J. P. *Nature* **1964**, *68–9*, 201.
26. Saini, P.; Choudhary P. *J. Nanoparticle Resea.* **2013**; doi: 10.1007/s11051-012-1415-2.
27. Olmedo, L.; Hourquebie, P.; Jousse, F. Handbook of Organic Conductive Molecules and Polymers; John Wiley & Sons Ltd: Chichester, **1997**.
28. Schulz, R. B.; Plantz, V. C.; Brush, D. R. *IEEE Trans.* **1988**, *30*, 187.
29. Saini, P.; Choudhary, V.; Singh, B. P.; Mathur, R. B.; Dhawan, S. K. *Mater. Chem. Phys.* **2009**, *113*, 919.
30. Colaneri, N. F.; Shackeltte, L. W. *IEEE Trans. Instrum. Meas.*. **1992**, *41*, 291.
31. Nicolson, A. M.; Ross, G. F. *IEEE Trans. Instrum. Meas.* **1970**, *19*, 377.
32. Weir, W. B. *Proc. IEEE* **1974**, *62*, 33.